An Ensemble Method for EEG-based Texture Discrimination during Open Eyes Active Touch

Andreas Miltiadous*
Department of Informatics and Telecommunications, University of Ioannina, Greece
a.miltiadous@uoi.gr

Vasileios Aspiotis*
Faculty of Medicine, University of Ioannina, Greece
v.aspiotis@uoi.gr

Dimitrios Peschos
Faculty of Medicine, University of Ioannina, Greece
dpeschos@uoi.gr

Katerina D. Tzimourta
Department of Electrical and Computer Engineering, University of Western Macedonia, Greece
ktzimourta@uowm.gr

Al Husein Sami Abosaleh
Open Lab, Newcastle University, UK
A.H.S.Abosaleh2@newcastle.ac.uk

Nikolaos Giannakeas
Department of Informatics and Telecommunications, University of Ioannina, Greece
giannakeas@uoi.gr

Alexandros T. Tzallas
Department of Informatics and Telecommunications, University of Ioannina, Greece
tzallas@uoi.gr (corresponding author)

** these authors contributed equally to this paper and share first authorship*

Received: 29 September 2023 | Revised: 12 October 2023 | Accepted: 15 October 2023

 DOI: https://doi.org/10.48084/etasr.6455

ABSTRACT

Touch sensation is a key modality that allows humans to understand and interact with their environment. More often than not, touch sensation depends on vision to accumulate and validate the received information. The ability to distinguish between materials and surfaces through active touch consists of a complex of neurophysiological operations. To unveil the functionality of these operations, neuroimaging and neurophysiological research tools are employed, with electroencephalography being the most used. In this paper, we attempt to distinguish between brain states when touching different natural textures (smooth, rough, and liquid). Recordings were obtained with a commercially available EEG wearable device. Time and frequency-based features were extracted, transformed with PCA decomposition, and an ensemble classifier combining Random Forest, Support Vector Machine, and Neural Network was utilized. High accuracy scores of 79.64% for the four-class problem and 89.34% for the three-class problem (Null-Rough-Water) were accordingly achieved. Thus, the methodology's robustness indicates its ability to classify different brain states under haptic stimuli.

Keywords-haptic; active touch; electroencephalogram; classification; multisensory; machine learning; PCA; ensemble method

I. INTRODUCTION

One of the basic human mechanisms for perceiving and exploring the surrounding world is the sense of touch. It is one of the earliest developed senses and plays a crucial role in daily tasks like object manipulation and action performance. Sensory loss of touch could lead to someone being unable to feel pain or temperature, missing the sense of presence, not being able to effortlessly move [1], and/or experience other atypical implications.

Acquiring information about the surroundings through touch requires physical contact and interaction between the surface of an object and the human skin, most commonly through the fingertips due to their high sensitivity. This contact results in the mechanical stimulation of the skin where mechanoreceptors transduce a nerve signal which is transferred through the peripheral nervous system pathways to the central nervous system and the brain. There, high order somatosensory areas, mainly the postcentral gyrus [2], are involved in the process of interpreting the signal. Information regarding the physical and geometric properties of the material, object, or surface being touched can be extracted. Such properties can be about the object's shape and size, the material substance and texture, hardness and elasticity, roughness, or temperature [2, 3]. This information analysis in the brain, integrated with proprioceptive, kinesthetic, cutaneous and thermal characteristics is called haptic perception. Haptic perception includes active and passive touch (tactile). The former occurs when human body parts are willingly used for exploration by moving against the surroundings while the latter is performed when outside agencies interact with static parts of the human skin [4]. Neural operations and perceptual differences between those two forms are still under investigation with numerous studies substantiating diversities in performance, in the activated brain area discrimination and in the neural response patterns involved [5-8]. Haptic perception is not limited to a fundamental ability of distinguishing different material properties. It is a subjective experience [9, 10] that has the capacity to create mental apprehension of the surroundings, both discriminatively and affectively [11]. Visual, auditory, and memory aspect incorporation complementarily contributes to constituting a multimodal system [9] that impacts the emotional, social and cognitive human apprehension [13-15]. Understanding the way human senses work, and more particularly how haptic perception functions has become a growing research topic over the recent years [13]. The importance and reasoning behind decoding haptic modality are driven by the numerous applications spotted in human psychology and physiology. Starting from the medical field with applications such as limb rehabilitation and assistive haptic robotics [16], neurophysiological disorder treatment [17], therapeutic interventions on tactile deficits in humans with mental disorders (anorexia nervosa) [18], and stroke rehabilitation [19], haptic perception understanding extends to most parts of human activity. The Industrial field makes use of the affective sensations through touch for manufacturing commercial products [20] like fabrics or clothes. Technological novelties, interface and application design utilize the knowledge on haptic perception to develop haptic interfaces [21], tactile displays, interactive media devices [22], and affective computing [23].

Non-invasive neuroimaging and neurophysiological methods including functional Magnetic Resonance Imaging (fMRI) and Electroencephalogram (EEG) enable researchers to examine the brain's response to touch stimuli. Especially the EEG portability, ease of use, low cost, and high temporal resolution, have generated novel experimental scenarios related to haptic sensation research. Corresponding studies implement analysis techniques such as Power Spectral Density [6, 24], event-related potentials [25], and somatosensory evoked potential [26-28]. In addition, advancements in machine learning technologies are combined with EEG analysis techniques to conclude in the classification of different brain states under haptic stimuli. These studies investigate discriminative touch and touch imagery [29, 30], roughness recognition classification [6, 31, 32], and tactile pleasantness in response to different textures or touch types [12, 33, 34]. Most studies examine active touch after eliminating the visual stimuli since it may have a major impact in haptic perception [35]. However, tactile perception in combination with visual stimuli has also been explored. Authors in [36] proposed a classification scheme for object shape recognition from EEG signals acquired with both tactile and visual stimuli. They used electrodes located on the frontal somato-sensory and occipital region that are responsible for the cognitive processing and the employment of Power Spectral Density and Mu-desynchronization.

In this research, we seek to address the multisensory nature of haptic perception and distinguish brain responses when touching different materials. Specifically, we propose a methodology for the discrimination of different natural material textures during active touch and constant visual contact through EEG signal classification. Multisensory stimuli can improve the classification accuracy more than conventional, single-sensory input [37]. Commonly, publications do not employ multiple machine learning algorithms for the classification procedure investigating active touch [6]. We designed an experimental protocol for EEG acquisition and preprocessing, then performed feature extraction, implemented Principal Component Analysis (PCA), and employed multiple classification algorithms for the EEG signal categorization under different haptic stimuli. Ultimately, we suggest an ensemble classification method that exceeds in performance every classifier tested.

II. MATERIALS AND METHODS

This section describes the stages of the proposed methodology. First, the experimental protocol for obtaining and preprocessing the EEG recordings is set out. Then, the procedure for extracting the features used for the classification of each active touch condition is explained, along with the dimensionality reduction of the feature matrix. Finally, the algorithms and the ensemble method used for performing the classification of the active touch states are described. Figure 1 represents a diagram of this experiment's entire methodology.

A. Dataset

The experimental procedure was held in a clinical, quiet and controlled environment. For this experiment, participants were asked to comfortably sit in a chair and a researcher explained them the procedure. They were given time to familiarize with the device and were instructed to relax during the experiment. Then, their right hand (dominant hand as validated with Edinburg Handedness Inventory [38]) was positioned in a fixed ergonomic arm support. The texture materials were visible while the participants were asked to use their right hand fingertips to softly rub each texture for one minute, in a circular, clockwise manner, without applying pressure on any material. The participants were asked to keep having visual contact with the material throughout the 1-minute active touch recording. In order to minimize the variance in movements and pressure applied, participants arms were fixed on the arm support with a rubber band and calibrated on their respective relative height horizontal to the surface position. An experienced researcher was always supervising the procedure.

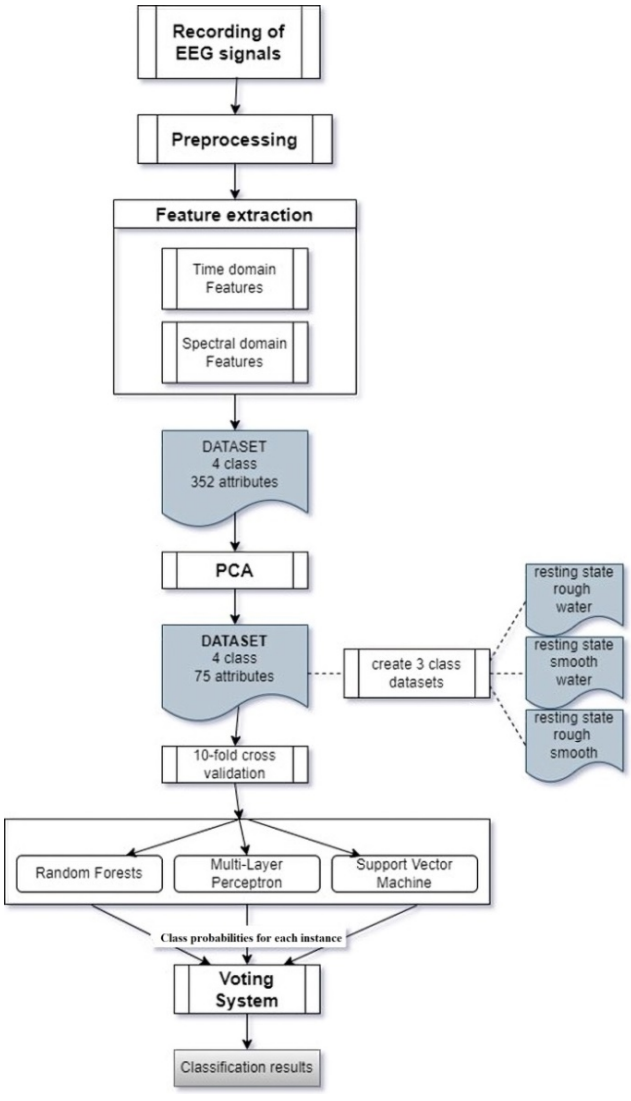

Fig. 1. Flowchart of the proposed methodology.

The protocol in brief steps:

1. 1-minute eyes-open resting-state recording.
2. 1-minute recording during active texture rubbing smooth surface.
3. 1-minute rest.
4. 1-minute recording during active texture rubbing rough surface.
5. 1-minute rest.
6. 1-minute recording during active texture touching liquid surface.

In total, 12 participants took part in the experiment, 7 males and 5 females. The participant age was between 25-27 years old. Every participant was right-handed with no history of neurological or psychiatric disorders. Detailed information about the procedure was given to every participant prior to the experiment by an experienced researcher. Written consent forms were obtained, ensuring that there was no concern regarding the experimental protocol and that their EEG recordings along with their private data could be used for publication purposes.The natural textures used in this study were: two materials of different roughness levels (smooth and rough) and liquid. For the smooth material, a satin polished stainless steel was employed with Ra < 0.5 μm (Roughness average). For the rough material, a piece of a 120 Grit sandpaper was used (estimated Ra = 1.32 μm. For the liquid surface, room temperature water (10^{-3} Pa.s.) in a shallow container was utilized. The Emotiv EPOC Flex wearable device was hired for the EEG data recording. This device is equipped with 32 gel Ag/AgCl sensors and a flexible cap. It is a portable headset with a rechargeable lithium battery and each electrode frequency response is 0.16-43 Hz, while the device sampling rate is 1024 Hz. The electrode placement was in accordance with the extended 10–20 International Reference System and 32 electrodes were positioned (Cz, Fz, Fp1, F7, F3, Fc1, C3, Fc5, T9, T7, Tp9, Cp5, Cp1, P3, P7, O1, PZ, OZ, O2, P8, P4, Cp2, Cp6, Tp10, T8, Fp10, Fc6, C4, Fc2, F4, F8, Fp2). Also 2 electrodes were placed on the ear lobes, namely A1 and A2. CMS and DRL electrodes were P3 and P4, respectively. The recording quality was constantly being ensured in real-time, by using the native EmotivBCI interface, which provides real-time information about electrode connectivity and signal quality. An experienced researcher continuously ensured that the electrode connection was at the best state according to the EmotivBCI interface, by reapplying gel on the electrodes if needed, so as every electrode impedance value would constantly be below the designated value (<20 kΩ). The recordings were streamed to a PC via a wireless connection to be saved and later processed. Figure 2 illustrates the materials used and the experimental procedure.

B. Data Preprocessing and Feature Extraction

The EEG recordings were digitally rereferenced to the average of A1, A2 electrodes which were placed at the left and right ear lobe, respectively. Recordings were downsampled from 1024 to 128 Hz during the wireless transmission stage. Furthermore, a 4th order Butterworth high-pass filter at 0.4 Hz

was applied. No low pass filter was set since the Emotiv EPOC Flex firmware automatically applies a double notch filter at 50 Hz and 60 Hz to remove interference from the electrical power supply. Also, Emotiv Flex has a built-in low-pass filter of 45 Hz [39]. The filter affects frequencies down to about 45 Hz, so the manufacturer specifies 43 Hz as the upper usable frequency limit where the spectral response is perfectly flat [40]. Next, artifacts of electrode movement were manually removed from visual inspection, in the EEGLAB MATLAB environment. No electrodes were removed from any of the EEG recordings, only time segments.

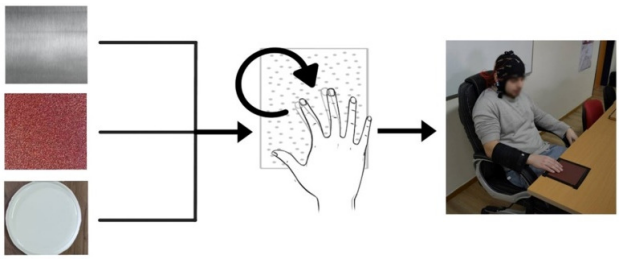

Fig. 2. The experimental protocol and the materials used: smooth, rough, liquid.

Subsequently, epoching of the EEG signals was performed. Signals were segmented into 1 s epochs with 0.5 s overlap. Epochs of 2 and 5 s were also extracted and the duration of 1 s was chosen based on the accuracy results. Afterwards, time and frequency domain metrics were extracted from each epoch to form the classification dataset. The time domain metrics were: Mean, Variance, Range, Median, Interquartile Range, 30% Percentiles. Frequency domain features were the Spectrum Power Density of each frequency band, for each epoch, calculated with the Power Spectral Density Welch method. The frequency bands were defined as [41]:

- Alpha: 8-12 Hz
- Beta: 12-25 Hz
- Theta: 4-8 Hz
- Delta: 1-4 Hz
- Gamma: 25-43 Hz

In total, 352 features were extracted (6 time domain and 5 spectral domain features for each of the 32 electrodes).

C. Dimensionality Reduction

PCA is a widely used method for dimensionality reduction in high-dimensional datasets. For a p-dimensional dataset, PCA analysis creates a p-dimensional vector of weights $w_{(k)} = (w_1, \dots, w_p)_{(k)}$ projecting each row vector $x_{(i)}$ to a new principal component score vector $t_{k(i)} = x_{(i)} * w_{(k)}$ for i =1,…., n and k = 1,….., p where n is the number of the individual recordings on the data [42]. To achieve the highest variance, the first principal component is computed so that the sum of each point squared distance is maximized. Then, each other principal component is calculated in order to have the maximum sum of squared values while being perpendicular to all its previous principal components. After calculating the principal component transformation, one can perform dimensionality reduction to the dataset by removing the components with the least variance. Thus, projecting a dataset of p-dimensional data to a dataset of r-dimensional data where $r < p$. In this experiment, the feature vector was standardized before the PCA transformation was calculated and then the less important principal components, which accounted for less than 5% of the total variance, were discarded (95% variance threshold). This way, the initial dataset of 352 features was converted to a linear transformation of 75 features. Figure 3 represents the PCA dimensionality reduction procedure followed in this dataset. PCA is implemented for reducing the feature space of the datasets capitalized by the classification algorithms, to achieve faster computational time and higher accuracy.

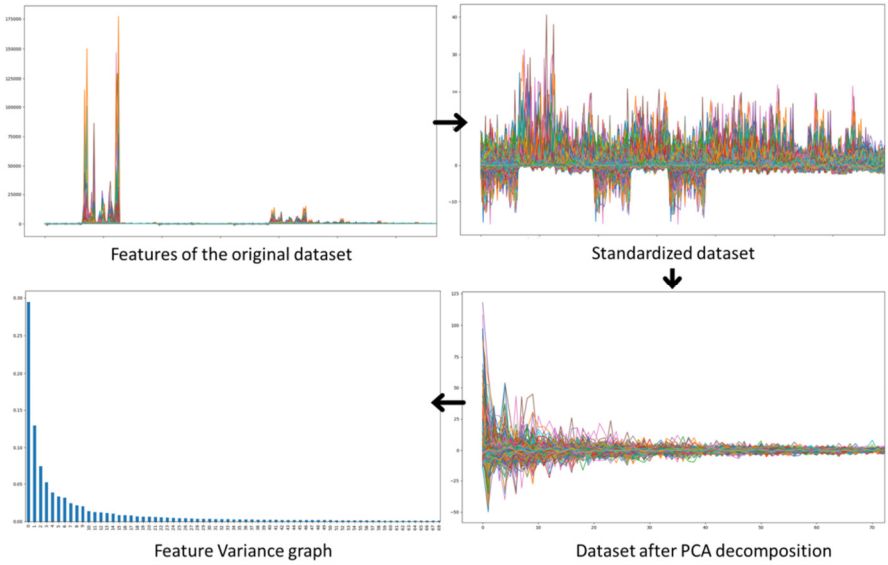

Fig. 3. Visual representation of the PCA stages: Original dataset, standardized dataset, principal component variances, PCA decomposition.

D. Classification

In this section, the utilized classification algorithm are described, those being: Random Forest (RF), k-Nearest Neighbor (k-NN), Multi-Layer Perceptron (MLP), C4.5 Decision Trees (DTs), Linear Discriminant Analysis (LDA), and Support Vector Machines (SVMs). The ensemble method is also presented. For each classification case, accuracy (ACC), sensitivity (SENS), and specificity (SPEC) scores were calculated. Equations (1)-(3) represent how ACC, SENS, and SPEC are computed for a binary problem. TP stands for True Positive, TN for True Negative, FP for False Positive, and FN for False Negative, respectively.

$$\text{ACC} = \frac{TP+TN}{TP+TN+FP+FN} \quad (1)$$

$$\text{SENS} = \frac{TP}{TP+FN} \quad (2)$$

$$\text{SPEC} = \frac{TN}{TN+FP} \quad (3)$$

To calculate these metrics in a multiclass problem, we averaged their scores in one versus all binary problems.

The four classes in the classification were:

1. Resting state or Null (N)
2. Rough (R)
3. Smooth (S)
4. Water (W)

These classes were combined in 4 classification problems:

1. N-R-S-W
2. N-S-W
3. N-R-W
4. N-R-S

The accuracy, sensitivity, and specificity scores of every classification problem were obtained by using the 10-fold validation method. Every classification algorithm and the ensemble method were employed in the Weka platform [43] while the hyperparameter optimization for each algorithm took place in Python, using the skopt.gp_minimize routine [44]. The Standard Deviation (SD) of the accuracy for each algorithm has been calculated after performing the classification routine 10 times.

E. C4.5 Decision Tree

DT algorithms are some of the most widely used methods for inductive inference [45]. C4.5 is an algorithm, first introduced by Ross Quinlan [46] that generates a DT robust to noisy data and capable of learning disjunctive expressions. The idea behind DT classification is to develop an if-else formula that can correctly determine an unknown instances class. The algorithm for producing a DT is quite simple. Beginning from the original training set, the information gain of each attribute - if split- is calculated. Then the attribute with the higher information gain value is selected and the tree is divided into subtrees based on this selected attribute. This procedure is repeated for each subtree until every element in the subset belongs to the same class or there are no more attributes to be selected. It should be noted that an attribute cannot be selected again as a partition attribute in the same subtree. To avoid overfitting, pruning techniques can be used. In this experiment, pruning by information gain in which a node is no longer expanded to a subtree and becomes a leaf based on a confidence factor was put to work. Reduced error pruning was employed as well, where a node is pruned if the resulting tree still has the same accuracy score as the unpruned version.

F. Random Forest

RF algorithm is an ensemble classifier [47, 57] and one of the most common techniques for classifying EEG data [48, 49]. This classifier involves multiple DTs, each of which uses a different subset of features as classification criteria and a different bootstrapped dataset (sampling with replacement) created from the original one as the training set. Then, each DT votes for each observation in the test set and the observation gets classified based on the average probability voting. Different weights can be given to each tree. This method employs the bagging idea to reduce the generalization error and improve classification accuracy. In this experiment, each tree was given the same weight. Moreover, no pruning of the created DTs was performed. The number of estimators to be used was obtained by the skopt.gp_minimize optimization pipeline in Python, which employs Bayesian Optimization utilizing Gaussian Processes, and found to be 110.

G. K-Nearest Neighbors

KNN algorithm classifies an instance of the test set by calculating its distance (Euclidean, Manhattan, etc.) from every instance in the training set while considering the majority class of the k-nearest ones [50]. In this experiment, k was set to 5 and the computed distance was Euclidean. The value of k was chosen after testing different k values from 1 to 10 and the one that produced the highest accuracy result was chosen.

H. Multi-Layer Perceptron

MLP is a commonly used feed forward Neural Network. An MLP consists of: an input layer with as many neurons as the dataset attributes, an output layer with as many neurons as the dataset classes, and one or more hidden layers. Each neuron receives multiple real-valued inputs and produces one real-valued output, determined by the activation function, usually being the sigmoid function. The gp_minimize pipeline was applied to calculate the learning rate which was found to be 0.32. Regarding the number of neurons and hidden layers, there are several methodologies for defining the optimal ones [51-53]. In this experiment, we used a trial-and-error technique to define the hidden layer size. Different hidden layer setups were implemented and finally it was decided to use one hidden layer with 39 neurons (the average of input plus output number of neurons).

I. Linear Discriminant Analysis

LDA is a dimensionality reduction technique that is also utilized as a classification method in many EEG classification problems [54] LDA aims to reduce the feature vector dimensionality by creating a new dimension that maximizes the

variance between each class. First the between-class scatter is calculated using equation 4.

$$S_b = \sum_{i=1}^{g} N_i(\overline{x_i} - \bar{x})(\overline{x_i} - \bar{x})^T \quad (4)$$

The within-class scatter is produced by calculating the covariance matrix of each class

$$cov_j = \left(x_j - \mu_j\right)\left(x_j - \mu_j\right)^T \quad (5)$$

and then by computing their average:

$$S_w = \sum_j p_j \times \left(cov_j\right) \quad (6)$$

The a priori probability of the class j , is p_j.

The LDA optimizing criterion is maximizing the S_b/S_w ratio. The transformed space axes are defined by maximizing this criterion. Once the LDA is completed, each data point of the test set is classified based on the smallest Euclidean distance from the class centers.

J. Support Vector Machines

A Support Vector Machine (SVM) is a machine learning algorithm that can solve binary classification problems. They have been widely encountered in biomedical applications and in EEG analysis [55, 58-60]. The SVM basic principle is to map the features to a high-dimensional feature space and locate an optimal separating hyperplane that maximizes the width of the gap between the two classes. To perform non-linear classification, an SVM can utilize the kernel method [56]. For multiclass classification such as the 4- or 3-class classification problems in this experiment, the classification problem is broken down into multiple two-class classification problems, in a one versus one approach. Additionally, in this experiment, the kernel function was a radial basis function. The kernel function selection was made after evaluating the performance results of every kernel function, namely linear, polynomial, radial basis, and sigmoid in the LibSVM implementation on the Weka platform [43].

K. The Ensemble Method

The proposed ensemble method is an average probability voting system consisting of the 3 best performing classification algorithms in this dataset: MLP, RF, and SVM. Initially, each classification algorithm is trained with the training set. For each instance of the test set, every classifier calculates the probability estimations for each class. Then the classifiers "vote" by averaging their probability estimations. The assigned class is the one with the higher average probability.

To examine the ensemble method's usefulness and check whether the employment of multiple classifiers with different architecture enhanced classification performance by eliminating the errors made by the classifiers, we conducted Mathiews correlation of errors between the individual classifiers and between the Ensemble Method with each classifier. To do so, the individual results of the classification were extracted while an array of 0 and 1 was created for each classifier, with 0 representing a classification error and 1 representing a correctly classified instance.

III. RESULTS

In the first classification problem, where all 4 experimental classes were used (Null, Rough, Smooth, Water), the voting system achieved a level of ACC of 79.64% (SENS=77.30%, SPEC=92.40%) outperforming the other classifiers and achieving the lowest SD of 2.19. MLP was the second best with 77.06% ACC followed by SVM (ACC 76.50%) and RF (ACC 70.86%). Table I illustrates the results of the N-R-S-W classification problem.

TABLE I. PERFORMANCE RESULTS FOR THE N-R-S-W CLASSIFICATION PROBLEM

Algorithm	ACC	SD	SENS	SPEC
Voting system	79.64%	2.19	77.30%	92.40%
RF	70.86%	2.32	70.80%	90.20%
DT	47.14%	2.83	47.10%	82.30%
KNN	64.90%	2.52	67.00%	89.00%
LDA	67.80%	2.35	67.80%	89.20%
SVM	76.50%	2.21	76.40%	92.10%
MLP	77.06%	2.33	77.00%	92.30%

In the second classification problem, where 3 experimental classes were considered (Null, Smooth, Water), the voting system achieved an ACC level of 87.67% (SENS=85.90%, SPEC=93%) outperforming all other classifiers while achieving the lowest SD (2). MLP was the second best with 84.70% ACC followed by SVM (ACC 84.50%) and LDA (81.10%). RF scored an ACC level of 79.30%. The rest of the classifiers achieved ACC lower than 72%. Table II shows the results of the N-S-W classification problem.

TABLE II. PERFORMANCE RESULTS FOR THE N-S-W CLASSIFICATION PROBLEM

Algorithm	ACC	SD	SENS	SPEC
DT	55.64%	3.64	57.10%	78.50%
RF	79.30%	2.51	79.60%	89.80%
KNN	71.22%	2.94	72.20%	86.00%
MLP	84.70%	2.34	84.80%	92.40%
LDA	81.10%	2.39	81.10%	90.50%
SVM	84.50%	2.26	84.50%	92.20%
Voting system	87.67%	2.00	85.90%	93.00%

In the third classification problem, 3 experimental classes were used (Null, Rough, Water). The voting system achieved an ACC level of 89.34% (SENS=85.90%, SPEC=93%) outperforming all other classifiers and achieving the lowest SD of 1.42. MLP was the second best with 86.50% ACC followed by SVM (ACC 86.30%), RF (82.56%), and LDA (82.25%). KNN achieved an accuracy level of 74.31% while DT performed the lowest, with an ACC score of 60.1%. Table III shows the results of the N-R-W classification problem.

TABLE III. PERFORMANCE RESULTS FOR THE N-R-W CLASSIFICATION PROBLEM

Algorithm	ACC	SD	SENS	SPEC
DT	60.10%	3.55	60.00%	80.00%
RF	82.56%	2.56	82.50%	91.20%
KNN	74.31%	3.37	77.10%	88.50%
MLP	86.50%	2.36	86.40%	92.00%
LDA	82.25%	2.22	82.10%	91.00%
SVM	86.30%	1.99	86.30%	92.10%
Voting system	89.34%	1.42	85.90%	93.00%

In the fourth classification problem, where three experimental classes were used (Null, Rough, Smooth), the voting system achieved an ACC level of 82.10% (SENS=79.80%, SPEC=89.9%) outperforming the other classifiers and achieving the lowest SD of 2.33. Nevertheless, it performed noticeably worse than in the other 3-class classification problems. SVM was the second best with 79.13% ACC followed by MLP (ACC 78.33%) and RF (75%). The other classifiers achieved accuracy lower than 72%. Table IV shows the scores of the N-R-S classification problem.

TABLE IV. PERFORMANCE RESULTS FOR THE N-R-S CLASSIFICATION PROBLEM

Algorithm	ACC	SD	SENS	SPEC
DT	54.27%	3.48	56.00%	78.00%
RF	75.00%	2.67	75.00%	87.40%
KNN	70.06%	3.27	71.40%	85.70%
MLP	78.33%	2.89	78.10%	89.00%
LDA	70.62%	2.74	70.60%	85.30%
SVM	79.13%	2.62	79.20%	89.60%
Voting system	82.10%	2.33	79.80%	89.90%

Figure 4 exhibits the comparison between the ACC scores of each classifier in the four classification problems. It can be noticed that, overall, the N-R-S-W problem achieved the lowest ACC scores, while the N-R-W problem achieved the highest ones. Concerning the 3-class problems, the performance in the N-R-S problem, was noticeably lower than in the others. Figure 5 represents the overall ACC, SENS and SPEC scores comparison among all the algorithms across all problems.

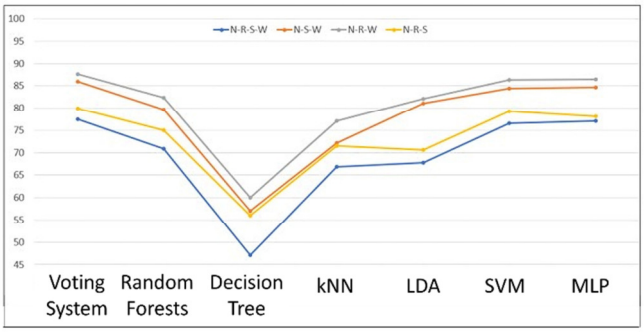

Fig. 4. All classification algorithm accuracy comparison.

To evaluate individual classifier contribution, the correlation of each classifier's error in-between them, and the correlation of each classifier's error with the ensemble method should be investigated. The Matthews correlation results are depicted in Table V. Low correlation between individual classifiers, along with higher correlation between the Ensemble Method and each classifier indicate that the classifiers do not misclassify the same instances and there is a benefit on using a combination of these classifiers (also based on the comparison of the performance results). Finally, to further investigate the performance of the proposed methodology for each classification problem, we calculated the Area Under Curve (ROC AUC) of each class versus the rest (OvR), along with the Precision Recall Curve (PRC) Area. The results are reported in Table VI.

TABLE V. CORRELATION OF ERRORS BETWEEN CLASSIFIERS

Mathiews correlation	SVM	MLP	RF	Voting system
SVM	---	0.33	0.4	0.75
MLP	0.33	---	0.3	0.564
RF	0.4	0.3	---	0.59

TABLE VI. AREA UNDER ROC AND PRC FOR EVERY CLASSIFICATION PROBLEM

Problem / Class	N-S-R-W		N-R-W		N-S-W		N-R-S	
	ROC	PRC	ROC	PRC	ROC	PRC	ROC	PRC
1	0.974	0.951	0.972	0.962	0.975	0.963	0.984	0.973
2	0.933	0.812	0.972	0.952	---	---	0.917	0.823
3	0.914	0.813	---	---	0.964	0.934	0.909	0.852
4	0.967	0.914	0.969	0.935	0.966	0.934	---	---
Average	0.947	0.872	0.971	0.95	0.968	0.944	0.937	0.883

IV. DISCUSSION

In this paper, a robust methodology for classifying EEG signals during active touch on different textures was implemented. The study consisted of four stages: experimental procedure, data acquisition, signal preprocessing, and classification. At the first stage, the participants were asked to touch actively 3 different materials while maintaining minimum arm movement and their brain function was recorded using an EEG wearable device. At the second stage, the EEG signal was preprocessed and different features were extracted which were later transformed using a PCA decomposition. Finally, this reformed feature dataset was used to train an ensemble classifier. The ensemble classifier consisted of a voting system of 3 distinct classifiers (RF, MLP, SVM), each of them utilizing a different classification principle. Finally, the proposed methodology was tested on 4 different classification problems and proved to be very effective since high accurate results were achieved.

In previous preliminary work on the same dataset, we observed that utilizing both temporal and spectral feature characteristics provided better classification accuracy in comparison to employing only spectral features [61]. However, other studies have highlighted that non-linear feature characteristics such as entropy [32] and determinism may also be useful for classifying active touch states considering the non-linear nature of brain signals and haptic perception entanglement. Table VII presents a list of previous works related to haptic task classification and the used methodology.

This research suggests that by using PCA feature reduction, the training and testing times are reduced while higher overall ACC is achieved. The voting system time performance was improved by 95% when PCA was applied. Particularly, the voting system's training time was 42 s in the 4-class classification problem. When training the voting system with the original non PCA-reduced dataset, the training time was 887 s. Similar time performance improvements were achieved in every classification problem. This is due to the fact that choosing the number of neurons in the neural network depends on the number of the dataset features. Therefore, by reducing the feature matrix from 353 to 75 features, both memory and time demands were decreased.

TABLE VII. COMPARISON WITH PREVIOUS WORKS

Reference	Year	Experimental protocol	Methodology	Classification problem	Results		
					ACC	SENS	SPEC
[32]	2020	Dynamic passive touch, rotating surface, roughness.	Features: Recurrence rate, determinism, LDA.	Rough, smooth, semi-rough.	93%	-	-
[31]	2021	Active touch, roughness, synthesized textured surfaces.	Deep learning CNN	Rough, smooth, semi-rough.	70%		
[6]	2019	Active touch, roughness, synthesized textured surfaces, different rubbing speeds (slow, medium, fast).	PSD, Features: Alpha and beta bands, time, SVM.	Flat, medium rough.	90.2%	83.3%	
[30]	2021	Active touch, haptic imagery, textures, finger slide	Features: Alpha and beta bands, common spatial pattern, LDA, event-related spectral pertubation analysis.	4 textures real touch, 4 textures imagery touch.	68% (real touch) 7.55% (imagery touch)		
[10]	2019	Affective tactile stimulation, 4 different fabrics, self assessment, arousal, valence	PSD, KNN.	Arousal, valence.	74.24%		
Proposed	2023	Active touch, fixed hand position, circular motion rubbing, 3 surfaces	Spectral and time features, PCA, ensemble method.	N-R-S-W	79.64%	77.30%	92.4%
				N-S-W	87.67%	85.9%	93%
				N-R-W	89.34%	85.90%	93%
				N-S-R	82.1%	79.8%	89.9%

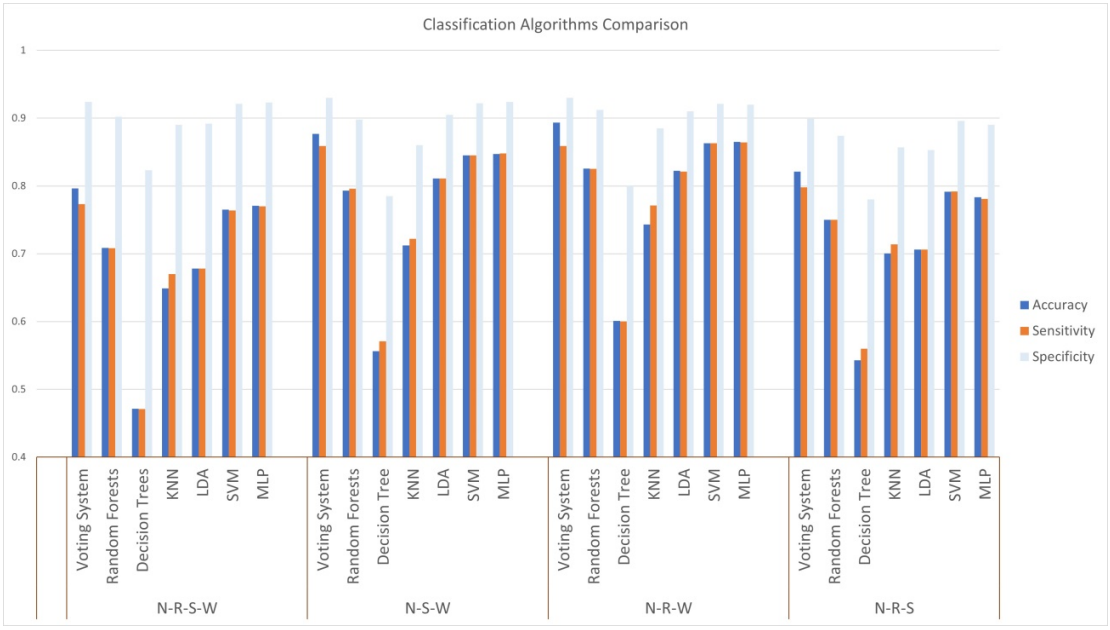

Fig. 5. ACC, SENS, SPEC scores of all algorithms across every problem.

Regarding how the PCA transformation can influence the classification performance, we can observe that the voting system ACC is significantly increased in all classification problems. The comparison of the ACC scores with and without PCA-transformed data is presented in Table VIII.

TABLE VIII. VOTING SYSTEM ACC RESULTS WITH AND WITHOUT PCA-TRANSFORMED DATASET

Classification problem	With PCA	Without PCA
N-R-S-W	79.64%	52.41%
N-S-W	87.67%	69.72%
N-R-W	89.34%	68.89%
N-R-S	82.10%	63.47%

The 3-class problem classifications were tested along with the 4-class problem classifications in order to examine whether their accuracy differences were significant. As expected, the 4-class problem classification problems achieved lower ACC scores. However, it can be observed that the classification ACC of the N-R-S problem (82.1%) is inferior to the N-R-W and N-S-W counterparts (87.67% and 89.34%, respectively), indicating a possible variation in the brain reception mechanisms triggered during the contact with a liquid surface. The utilized voting system proved to be effective since its classification performance was consistently higher than that of individually employed SVM, RF, and MLP. Specifically, in all classification problems, the voting system achieved 0.5% to 3.5% higher ACC while maintaining lower SD scores. To further validate that the ensemble method provides better

performance in comparison to the other algorithms (especially SVM), we conducted independent sample T-tests between the ACC results of the SVM algorithm (10 runs) and the ensemble method (10-runs) for each classification problem. The performance difference for all the problems was statistically significant, with every p-value <0.001.

The scope of this research was to classify the different active touch states while performing a predetermined hand movement and having visual contact with the texture. Other studies have tried to identify distinct brain behavior under different haptic stimuli [34, 62, 63]. However, no specific protocol has been established regarding the experimental procedure during the signal acquisition. The elaborate nature of haptic perception and the complex functionality of cutaneous and kinesthetic mechanoreceptors have allowed researchers to employ a wide range of approaches and tools. In the majority of the other studies, the experimental protocol about hand movement is extensively controlled. For example, authors in [32] had the participants place their hands in a completely motionless state, while authors in [30] allowed only a finger slide. Furthermore, almost every study regarding haptic perception has the participants keeping their eyes closed during the experiment. Depending on the scope of research there is a focus on the exploration control, attempting to isolate the stimuli. According to [4], the distinction between active and passive experimental procedures can be questioned on whether the active approaches are truly active. Our study allowed an adequate degree of freedom on the finger motion while restraining any hand and arm movement along with maintaining visual contact with the material. By doing so, we attempt to simulate a natural approach of a human exploring a surface in a quest to identify its characteristics. Moreover, contrary to other research approaches that use only specific brain regions or feature selection methods for keeping the dataset dimensionality low, we choose not to dismiss information of the perplexed neural connections but to perform, instead, the dimensionality reduction through a PCA decomposition process. We achieved an ACC score of 79.64% for a 4-class problem and an 89.34% for a 3-class problem in our classification between all subjects with all the electrodes available and not at a single-subject level classification. Thus, direct comparison with other research cannot be performed, mainly because of the dissimilarities in the experimental protocol and the differences in the classification approach.

The brain mechanisms have the ability to get acquainted to a continuous stimulus. This may lead this classification routine to reduced performance if the participant is exposed to the stimuli for too long. Although this classification protocol was strict considering the time duration of the experiments, it should be examined whether there are significant changes in the EEG features exported right after the stimuli induction with the EEG features exported after the brain had already got familiar with the stimuli. We examined whether there was a performance drop when using tactile perception EEG signals that have been recorded after a certain duration of activity, in two ways. First, we split the feature dataset in two subsets. The first one containing the former 30 time windows of each recording (30 × 1 s epochs). The latter containing the last 30 time windows. We performed the 4-class classification pipeline 10 times. The ACC score of the first group of epochs at average was 78.75% and the ACC of the second was 80.18%. Independent sample T-test was carried out and the difference in performance was not found to be statistically important, meaning that this classification problem is not time dependent. However, this should be further validated by obtaining longer EEG recordings. Also, an independent T-test was employed between the features of each participant at every state (resting state, rough, smooth, water). Every test with p-value less than 0.05 was classified as 1 (statistically significant differences) and every test with p-value bigger than 0.05 was classified as 0. For every participant, the percentage of features that presented statistically important differences at each state was calculated. It was observed that: (1) even in the resting state recordings, 27.8% of the features had significant changes without an obvious cause. (2) Regarding the tactile perception recordings, 21-26.4% of the features had significant changes. Table IX represents the percentages of features that presented statistically important changes between the 2 states along with the difference percentage between the resting state and the active state. In total, more than 75% of the features did not present statistically important changes, which indicates that this model is not strongly time-dependent.

TABLE IX. PERCENTAGE OF FEATURES WITH STATISTICAL IMPORTANT CHANGES, FOR EVERY PARTICIPANT, BETWEEN THE FIRST 30 S AND THE LAST 30 S OF A RECORDING

	% Statistical important changes				**% Difference of resting state with tactile perception**
Participant	**Rest**	**Rough**	**Smooth**	**Water**	
1	0.193	0.196	0.161	0.187	0.011
2	0.235	0.068	0.215	0.400	0.007
3	0.264	0.207	0.130	0.241	0.071
4	0.298	0.463	0.420	0.295	-0.094
5	0.420	0.153	0.406	0.326	0.125
6	0.156	0.215	0.326	0.244	-0.106
7	0.468	0.153	0.252	0.190	0.269
8	0.082	0.491	0.073	0.204	-0.174
9	0.156	0.318	0.497	0.093	-0.146
10	0.389	0.159	0.181	0.230	0.198
11	0.409	0.119	0.230	0.366	0.170
12	0.264	0.059	0.176	0.392	0.054
Average	0.278	0.217	0.256	0.264	0.032

The limitations of this methodology should be addressed. To begin with, increasing the EEG recording should produce more accurate and generalizable results. Also, analyzing the neurophysiological brain activity during the experiment could lead to a better understanding of the interaction between specific brain regions and possible result in a more elaborate feature extraction procedure. In addition, considering the degrees of freedom in the finger movement, the classification procedure may be affected by the individual's way of interaction. Conscious or unconscious decisions made by individuals regarding speed, strength, and muscle movement may affect the joint and muscle mechanoreceptor activity. Finally, the non-randomized experimental protocol of this experiment can be considered a limitation, because of the uncertainty of whether the order of the trials may enhance or reduce the classification accuracy due to mental factors such as fatigue. However, randomizing the trial order could lead to other limitations such as the non-repeatability of the experiment or, in the case of the water trial, preceding the smooth or rough trial, moisture remaining on the hand may affect the EEG signal. Thus, we considered the non-randomized protocol as our best option.

Nevertheless, the above limitations regarding the motor movement and the cognitive brain function during the active touch are to be leveraged in our future work. We intend to dissociate visual-to-haptic combination by exploring the differences of eyes-open and eyes-closed haptic exploration. Additionally, the next stage of this research will aim to explore the imagery aspects of active touch when using virtual reality and head mounted displays. Future work could indicate whether visual and cognitive touch imagery could be distinguished without actual touching within virtual reality environments. Moreover, the communication patterns between brain regions during haptic stimulus are to be explored in that sense.

V. CONCLUSIONS

In this paper, a technique for categorizing EEG signals during active contact, obtaining notable accuracy in a variety of categorization settings is proposed. To achieve high accuracies of 79.64% for the N-R-S-W problem, 87.67% for the N-S-W problem, 89.34% for the N-R-W problem, and 82.1% for the N-R-S problem, we strategically integrated SVM, MLP, and RF algorithms through an ensemble method. We used PCA to reduce the number of features, which not only sped up computation but also improved the precision and robustness of our classifications. Importantly, our results confirmed the time-independence of the categorization approach, demonstrating its endurance over extended time. This robustness highlights our method potential for more extensive applications when combined with our ensemble methodology. These findings can have a wide range of applications. Our study has possible implications in prosthetics, robotics, and communication restoration in addition to advancing our understanding of EEG-based tactile discrimination, especially given its proven stability and precision.

CONFLICT OF INTEREST

The authors declare that the current research was conducted in the absence of any commercial or financial relationships that could be construed as a potential conflict of interest.

ACKNOWLEDGMENT

We acknowledge the support of this work by the project "Immersive Virtual, Augmented and Mixed Reality Center Of Epirus" (MIS 5047221) which is implemented under the Action "Reinforcement of the Research and Innovation Infrastructure", funded by the Operational Program "Competitiveness, Entrepreneurship and Innovation" (NSRF 2014-2020) and co-financed by Greece and the European Union (European Regional Development Fund).

REFERENCES

[1] G. Robles-De-La-Torre, "The importance of the sense of touch in virtual and real environments," *IEEE MultiMedia*, vol. 13, no. 3, pp. 24–30, Jul. 2006, https://doi.org/10.1109/MMUL.2006.69.

[2] C. Reed and M. Ziat, "Haptic Perception: From the Skin to the Brain," in *Reference Module in Neuroscience and Biobehavioral Psychology*, Amsterdam, Netherlands: Elsevier, 2018, pp. 545–556.

[3] A. Gallace and C. Spence, "Touch and the body: The role of the somatosensory cortex in tactile awareness," *Psyche: An Interdisciplinary Journal of Research on Consciousness*, vol. 16, no. 1, pp. 30–67, 2010.

[4] M. A. Symmons, B. L. Richardson, D. B. Wuillemin, and G. H. VanDoorn, "Active versus passive touch in three dimensions," in *First Joint Eurohaptics Conference and Symposium on Haptic Interfaces for Virtual Environment and Teleoperator Systems. World Haptics Conference*, Pisa, Italy, Mar. 2005, pp. 108–113, https://doi.org/10.1109/WHC.2005.20.

[5] C. Simoes-Franklin, T. A. Whitaker, and F. N. Newell, "Active and passive touch differentially activate somatosensory cortex in texture perception," *Human Brain Mapping*, vol. 32, no. 7, pp. 1067–1080, Jul. 2010, https://doi.org/10.1002/hbm.21091.

[6] S. Eldeeb, J. Ting, D. Erdogmus, D. Weber, and M. Akcakaya, "EEG-Based Texture Classification During Active Touch," in *29th International Workshop on Machine Learning for Signal Processing*, Pittsburgh, PA, USA, Oct. 2019, pp. 1–6, https://doi.org/10.1109/MLSP.2019.8918777.

[7] A. Moungou, E. Vezzoli, C. Lombart, B. Lemaire-Semail, J.-L. Thonnard, and A. Mouraux, "A novel method using EEG to characterize the cortical processes involved in active and passive touch," in *Haptics Symposium*, Philadelphia, PA, USA, Apr. 2016, pp. 205–210, https://doi.org/10.1109/HAPTICS.2016.7463178.

[8] G. Anuradha and D. N. Jamal, "Classification of Dementia in EEG with a Two-Layered Feed Forward Artificial Neural Network," *Engineering, Technology & Applied Science Research*, vol. 11, no. 3, pp. 7135–7139, Jun. 2021, https://doi.org/10.48084/etasr.4112.

[9] S. Lederman and R. Klatzky, "TuTorial Review: Haptic Perception: A Tutorial," *Attention, perception & psychophysics*, vol. 71, no. 7, pp. 1439–1459, Oct. 2009, https://doi.org/10.3758/APP.71.7.1439.

[10] A. Greco, A. Guidi, M. Bianchi, A. Lanata, G. Valenza, and E. P. Scilingo, "Brain Dynamics Induced by Pleasant/Unpleasant Tactile Stimuli Conveyed by Different Fabrics," *IEEE Journal of Biomedical and Health Informatics*, vol. 23, no. 6, pp. 2417–2427, Aug. 2019, https://doi.org/10.1109/JBHI.2019.2893324.

[11] F. McGlone, J. Wessberg, and H. Olausson, "Discriminative and Affective Touch: Sensing and Feeling," *Neuron*, vol. 82, no. 4, pp. 737–755, May 2014, https://doi.org/10.1016/j.neuron.2014.05.001.

[12] H. Singh *et al.*, "The brain's response to pleasant touch: an EEG investigation of tactile caressing," *Frontiers in Human Neuroscience*, vol. 8, 2014, Art. no. 893, https://doi.org/10.3389/fnhum.2014.00893.

[13] H. Alsuradi, W. Park, and M. Eid, "EEG-Based Neurohaptics Research: A Literature Review," *IEEE Access*, vol. 8, pp. 49313–49328, 2020, https://doi.org/10.1109/ACCESS.2020.2979855.

[14] M. T. Fairhurst, F. McGlone, and I. Croy, "Affective touch: a communication channel for social exchange," *Current Opinion in Behavioral Sciences*, vol. 43, pp. 54–61, Feb. 2022, https://doi.org/10.1016/j.cobeha.2021.07.007.

[15] N. V. Kimmatkar and B. V. Babu, "Human Emotion Detection with Electroencephalography Signals and Accuracy Analysis Using Feature Fusion Techniques and a Multimodal Approach for Multiclass Classification," *Engineering, Technology & Applied Science Research*, vol. 12, no. 4, pp. 9012–9017, Aug. 2022, https://doi.org/10.48084/etasr.5073.

[16] A. Gutierrez, D. Sepulveda-Munoz, A. Gil-Agudo, and A. de los Reyes Guzman, "Serious Game Platform with Haptic Feedback and EMG Monitoring for Upper Limb Rehabilitation and Smoothness Quantification on Spinal Cord Injury Patients," *Applied Sciences*, vol. 10, no. 3, Jan. 2020, Art. no. 963, https://doi.org/10.3390/app10030963.

[17] A. C. Voos, K. A. Pelphrey, and M. D. Kaiser, "Autistic traits are associated with diminished neural response to affective touch," *Social Cognitive and Affective Neuroscience*, vol. 8, no. 4, pp. 378–386, Apr. 2013, https://doi.org/10.1093/scan/nss009.

[18] M. Grunwald, C. Ettrich, B. Assmann, A. Dahne, and W. Krause, "Deficits in haptic perception and right parietal theta power changes in patients with anorexia nervosa before and after weight gain," *International Journal of Eating Disorders*, vol. 29, no. 4, pp. 417–428, 2001, https://doi.org/10.1002/eat.1038.

[19] X. Hou and O. Sourina, "Emotion-enabled haptic-based serious game for post stroke rehabilitation," in *19th ACM Symposium on Virtual Reality Software and Technology*, Singapore, Asia, Oct. 2013, pp. 31–34, https://doi.org/10.1145/2503713.2503738.

[20] B. Hughes, J. Wang, D. Rosic, and K. Palmer, "Texture Gradients and Perceptual Constancy under Haptic Exploration," in *Second Joint EuroHaptics Conference and Symposium on Haptic Interfaces for Virtual Environment and Teleoperator Systems*, Tsukuba, Japan, Mar. 2007, pp. 66–71, https://doi.org/10.1109/WHC.2007.109.

[21] S. Biswas and Y. Visell, "Haptic Perception, Mechanics, and Material Technologies for Virtual Reality," *Advanced Functional Materials*, vol. 31, Feb. 2021, Art. no. 2008186, https://doi.org/10.1002/adfm.202008186.

[22] D. Prattichizzo, C. Pacchierotti, S. Cenci, K. Minamizawa, and G. Rosati, "Using a Fingertip Tactile Device to Substitute Kinesthetic Feedback in Haptic Interaction," in *International Conference on Human Haptic Sensing and Touch Enabled Computer Applications*, Amsterdam, Netherlands, Jul. 2010, pp. 125–130, https://doi.org/10.1007/978-3-642-14064-8_19.

[23] B. Petreca, N. Bianchi-Berthouze, S. Baurley, P. Watkins, and D. Atkinson, "An Embodiment Perspective of Affective Touch Behaviour in Experiencing Digital Textiles," in *Humaine Association Conference on Affective Computing and Intelligent Interaction*, Geneva, Switzerland, Sep. 2013, pp. 770–775, https://doi.org/10.1109/ACII.2013.143.

[24] A. Miltiadous, E. Gionanidis, K. D. Tzimourta, N. Giannakeas, and A. T. Tzallas, "DICE-Net: A Novel Convolution-Transformer Architecture for Alzheimer Detection in EEG Signals," *IEEE Access*, vol. 11, pp. 71840–71858, 2023, https://doi.org/10.1109/ACCESS.2023.3294618.

[25] S. Ballesteros, F. Munoz, M. Sebastian, B. Garcia, and J. M. Reales, "ERP evidence of tactile texture processing: Effects of roughness and movement," in *Third Joint EuroHaptics conference and Symposium on Haptic Interfaces for Virtual Environment and Teleoperator Systems*, Salt Lake City, UT, USA, Mar. 2009, pp. 166–171, https://doi.org/10.1109/WHC.2009.4810901.

[26] C. Genna, C. Oddo, C. Fanciullacci, C. Chisari, S. Micera, and F. Artoni, "Bilateral cortical representation of tactile roughness," *Brain Research*, vol. 1699, pp. 79–88, Nov. 2018, https://doi.org/10.1016/j.brainres.2018.06.014.

[27] C. Genna, F. Artoni, C. Fanciullacci, C. Chisari, C. M. Oddo, and S. Micera, "Long-latency components of somatosensory evoked potentials during passive tactile perception of gratings," in *38th Annual International Conference of the IEEE Engineering in Medicine and Biology Society*, Orlando, FL, USA, Aug. 2016, pp. 1648–1651, https://doi.org/10.1109/EMBC.2016.7591030.

[28] A. Moungou, J.-L. Thonnard, and A. Mouraux, "Using EEG (SS-EPs) to characterize the brain activity in response to textured stimuli in passive touch," in *IEEE World Haptics Conference*, Evanston, IL, USA, Jun. 2015, pp. 113–118, https://doi.org/10.1109/WHC.2015.7177700.

[29] J.-H. Cho, J.-H. Jeong, M.-K. Kim, and S.-W. Lee, "Towards Neurohaptics: Brain-Computer Interfaces for Decoding Intuitive Sense of Touch," in *9th International Winter Conference on Brain-Computer Interface*, Gangwon, Korea, Feb. 2021, pp. 1–5, https://doi.org/10.1109/BCI51272.2021.9385331.

[30] M.-K. Kim, J.-H. Cho, and J.-H. Jeong, "Classification of Tactile Perception and Attention on Natural Textures from EEG Signals," in *9th International Winter Conference on Brain-Computer Interface*, Gangwon, Korea, Feb. 2021, pp. 1–5, https://doi.org/10.1109/BCI51272.2021.9385296.

[31] O. Ozdenizci, S. Eldeeb, A. Demir, D. Erdogmus, and M. Akcakaya, "EEG-based texture roughness classification in active tactile exploration with invariant representation learning networks," *Biomedical Signal Processing and Control*, vol. 67, May 2021, Art. no. 102507, https://doi.org/10.1016/j.bspc.2021.102507.

[32] G. Baghdadi, M. Amiri, E. Falotico, and C. Laschi, "Recurrence quantification analysis of EEG signals for tactile roughness discrimination," *International Journal of Machine Learning and Cybernetics*, vol. 12, no. 4, pp. 1115–1136, Apr. 2021, https://doi.org/10.1007/s13042-020-01224-1.

[33] A. Greco, M. Nardelli, M. Bianchi, G. Valenza, and E. P. Scilingo, "Recognition of affective haptic stimuli conveyed by different fabrics sing EEG-based sparse SVM," in *3rd International Forum on Research and Technologies for Society and Industry*, Modena, Italy, Sep. 2017, pp. 1–5, https://doi.org/10.1109/RTSI.2017.8065933.

[34] M. A. Becerra *et al.*, "Electroencephalographic Signals and Emotional States for Tactile Pleasantness Classification," in *International Workshop on Artificial Intelligence and Pattern Recognition*, Havana, Cuba, Sep. 2018, pp. 309–316, https://doi.org/10.1007/978-3-030-01132-1_35.

[35] N. Katsuyama, E. Kikuchi-Tachi, N. Usui, H. Yoshizawa, A. Saito, and M. Taira, "Effect of Visual Information on Active Touch During Mirror Visual Feedback," *Frontiers in human neuroscience*, vol. 12, Jan. 2018, Art. no. 424, https://doi.org/10.3389/fnhum.2018.00424.

[36] A. Khasnobish, A. Konar, D. N. Tibarewala, S. Bhattacharyya, and R. Janarthanan, "Object Shape Recognition from EEG Signals during Tactile and Visual Exploration," in *International Conference on Pattern Recognition and Machine Intelligence*, Kolkata, India, Dec. 2013, pp. 459–464, https://doi.org/10.1007/978-3-642-45062-4_63.

[37] W. Li, Q. Xu, Y. Li, C. Li, F. Wu, and L. Ji, "EEG characteristics in 'eyes-open' versus 'eyes-closed' condition during vibrotactile stimulation," *Biomedical Signal Processing and Control*, vol. 68, Jul. 2021, Art. no. 102759, https://doi.org/10.1016/j.bspc.2021.102759.

[38] J. F. Veale, "Edinburgh Handedness Inventory – Short Form: A revised version based on confirmatory factor analysis," *Laterality*, vol. 19, no. 2, pp. 164–177, Mar. 2014, https://doi.org/10.1080/1357650X.2013.783045.

[39] N. S. Williams, G. M. McArthur, B. de Wit, G. Ibrahim, and N. A. Badcock, "A validation of Emotiv EPOC Flex saline for EEG and ERP research," *PeerJ*, vol. 8, Aug. 2020, Art. no. e9713, https://doi.org/10.7717/peerj.9713.

[40] "Follow why does Emotiv EPOC+ stop at 43 Hz in range? Is there a way to expand this somehow?," *EMOTIV*, Dec. 12, 2018. https://www.emotiv.com/knowledge-base/follow-why-does-emotiv-epoc-stop-at-43-hz-in-range-is-there-a-way-to-expand-this-somehow/.

[41] J. J. Newson and T. C. Thiagarajan, "EEG Frequency Bands in Psychiatric Disorders: A Review of Resting State Studies," *Frontiers in Human Neuroscience*, vol. 12, Jan. 2019, Art. no. 521, https://doi.org/10.3389/fnhum.2018.00521.

[42] H. Abdi and L. J. Williams, "Principal component analysis," *WIREs Computational Statistics*, vol. 2, no. 4, pp. 433–459, 2010, https://doi.org/10.1002/wics.101.

[43] I. H. Witten, E. Frank, L. E. Trigg, M. A. Hall, G. Holmes, and S. J. Cunningham, "Weka: Practical machine learning tools and techniques with Java implementations," Working Paper, Aug. 1999. [Online]. Available: https://researchcommons.waikato.ac.nz/handle/10289/1040.

[44] T. Head, M. Kumar, H. Nahrstaedt, G. Louppe, and I. Shcherbatyi, "scikit-optimize/scikit-optimize." Zenodo, Jul. 12, 2021, https://doi.org/10.5281/zenodo.5565057.

[45] K. Polat and S. Gunes, "Classification of epileptiform EEG using a hybrid system based on decision tree classifier and fast Fourier transform," *Applied Mathematics and Computation*, vol. 187, no. 2, pp. 1017–1026, Apr. 2007, https://doi.org/10.1016/j.amc.2006.09.022.

[46] S. Ruggieri, "Efficient C4.5 [classification algorithm]," *IEEE Transactions on Knowledge and Data Engineering*, vol. 14, no. 2, pp. 438–444, Mar. 2002, https://doi.org/10.1109/69.991727.

[47] L. Breiman, "Random Forests," *Machine Learning*, vol. 45, no. 1, pp. 5–32, Oct. 2001, https://doi.org/10.1023/A:1010933404324.

[48] K. D. Tzimourta *et al.*, "A robust methodology for classification of epileptic seizures in EEG signals," *Health and Technology*, vol. 9, no. 2, pp. 135–142, Mar. 2019, https://doi.org/10.1007/s12553-018-0265-z.

[49] M. A. Alsuwaiket, "Feature Extraction of EEG Signals for Seizure Detection Using Machine Learning Algorthims," *Engineering, Technology & Applied Science Research*, vol. 12, no. 5, pp. 9247–9251, Oct. 2022, https://doi.org/10.48084/etasr.5208.

[50] M. Saeedi, A. Saeedi, and A. Maghsoudi, "Major depressive disorder assessment via enhanced k-nearest neighbor method and EEG signals," *Physical and Engineering Sciences in Medicine*, vol. 43, no. 3, pp. 1007–1018, Sep. 2020, https://doi.org/10.1007/s13246-020-00897-w.

[51] K. G. Sheela and S. N. Deepa, "Review on Methods to Fix Number of Hidden Neurons in Neural Networks," *Mathematical Problems in Engineering*, vol. 2013, Jun. 2013, Art. no. e425740, https://doi.org/10.1155/2013/425740.

[52] I. Tsoulos, D. Gavrilis, and E. Glavas, "Neural network construction and training using grammatical evolution," *Neurocomputing*, vol. 72, no. 1, pp. 269–277, Dec. 2008, https://doi.org/10.1016/j.neucom.2008.01.017.

[53] J. Heaton, *Artificial Intelligence for Humans: Deep Learning and Neural Networks*. Scotts Valley, CA, USA: CreateSpace Independent, 2015.

[54] R. Fu, Y. Tian, T. Bao, Z. Meng, and P. Shi, "Improvement Motor Imagery EEG Classification Based on Regularized Linear Discriminant Analysis," *Journal of Medical Systems*, vol. 43, no. 6, May 2019, Art. no. 169, https://doi.org/10.1007/s10916-019-1270-0.

[55] K. D. Tzimourta, L. G. Astrakas, M. G. Tsipouras, N. Giannakeas, A. T. Tzallas, and S. Konitsiotis, "Wavelet Based Classification of Epileptic Seizures in EEG Signals," in *30th International Symposium on Computer-Based Medical Systems*, Thessaloniki, Greece, Jun. 2017, pp. 35–39, https://doi.org/10.1109/CBMS.2017.116.

[56] J. Breneman, "Kernel Methods for Pattern Analysis," *Technometrics*, vol. 47, no. 2, pp. 237–238, May 2005, https://doi.org/10.1198/tech.2005.s264.

[57] A. Lahouar and J. Ben Hadj Slama, "Day-ahead load forecast using random forest and expert input selection," *Energy Conversion and Management*, vol. 103, pp. 1040–1051, Oct. 2015, https://doi.org/10.1016/j.enconman.2015.07.041.

[58] R. Chatterjee and T. Bandyopadhyay, "EEG Based Motor Imagery Classification Using SVM and MLP," in *2nd International Conference on Computational Intelligence and Networks*, Bhubaneswar, India, Jan. 2016, pp. 84–89, https://doi.org/10.1109/CINE.2016.22.

[59] A. Miltiadous *et al.*, "Alzheimer's Disease and Frontotemporal Dementia: A Robust Classification Method of EEG Signals and a Comparison of Validation Methods," *Diagnostics*, vol. 11, no. 8, Aug. 2021, Art. no. 1437, https://doi.org/10.3390/diagnostics11081437.

[60] P. Christodoulides *et al.*, "Classification of EEG signals from young adults with dyslexia combining a Brain Computer Interface device and an Interactive Linguistic Software Tool," *Biomedical Signal Processing and Control*, vol. 76, Jul. 2022, Art. no. 103646, https://doi.org/10.1016/j.bspc.2022.103646.

[61] V. Aspiotis *et al.*, "Active touch classification using EEG signals," in *6th South-East Europe Design Automation, Computer Engineering, Computer Networks and Social Media Conference*, Preveza, Greece, Sep. 2021, pp. 1–5, https://doi.org/10.1109/SEEDA-CECNSM53056.2021.9566257.

[62] H. Alsuradi and M. Eid, "Trial-based Classification of Haptic Tasks Based on EEG Data," in *IEEE World Haptics Conference*, Montreal, QC, Canada, Jul. 2021, pp. 37–42, https://doi.org/10.1109/WHC49131.2021.9517230.

[63] H. Alsuradi, C. Pawar, W. Park, and M. Eid, "Detection of Tactile Feedback on Touch-screen Devices using EEG Data," in *IEEE Haptics Symposium*, Crystal City, VA, USA, Mar. 2020, pp. 775–780, https://doi.org/10.1109/HAPTICS45997.2020.ras.HAP20.16.8d90d0bd.